Biochemical and Biophysical Research Communications 438 (2013) 588–593

Contents lists available at ScienceDirect

Biochemical and Biophysical Research Communications

journal homepage: www.elsevier.com/locate/ybbrc

Three-dimensional structure of a *Bombyx mori* Omega-class glutathione transferase

Kohji Yamamoto [a,*], Mamoru Suzuki [b], Akifumi Higashiura [b], Atsushi Nakagawa [b]

[a] Faculty of Agriculture, Kyushu University Graduate School, 6-10-1 Hakozaki, Higashi-ku, Fukuoka 812-8581, Japan
[b] Institute for Protein Research, Osaka University, Suita 565-0871, Japan

ARTICLE INFO

Article history:
Received 30 July 2013
Available online 11 August 2013

Keywords:
Crystal structure
Glutathione
Glutathione transferase
Lepidoptera
Site-directed mutagenesis

ABSTRACT

Glutathione transferases (GSTs) are major phase II detoxification enzymes that play central roles in the defense against various environmental toxicants as well as oxidative stress. Here we report the crystal structure of an Omega-class glutathione transferase of *Bombyx mori*, bmGSTO, to gain insight into its catalytic mechanism. The structure of bmGSTO complexed with glutathione determined at a resolution of 2.5 Å reveals that it exists as a dimer and is structurally similar to Omega-class GSTs with respect to its secondary and tertiary structures. Analysis of a complex between bmGSTO and glutathione showed that bound glutathione was localized to the glutathione-binding site (G-site). Site-directed mutagenesis of bmGSTO mutants indicated that amino acid residues Leu62, Lys65, Lys77, Val78, Glu91 and Ser92 in the G-site contribute to catalytic activity.

1. Introduction

Glutathione transferases [GSTs, EC 2.5.1.18] are ubiquitously expressed and are responsible for the intracellular detoxification of diverse xenobiotics and endogenous substances by conjugation them to reduced glutathione (GSH) [1,2]. Multiple classes of GSTs, including the Alpha, Mu, Pi, Omega, Sigma, Theta, and Zeta classes in mammals, are defined according to amino acid sequence differences [3]. Moreover, Delta, Epsilon, Omega, Sigma, Theta, and Zeta classes are present in dipteran insects such as *Anopheles gambiae* and *Drosophila melanogaster* [4].

Insect GSTs are particularly interesting because of their role in insecticide metabolism. In Lepidoptera, the Delta, Omega, Sigma, Zeta-class and unclassified GSTs of the silkworm *Bombyx mori* have been characterized [5–10]. Recently, the three-dimensional structures of a *B. mori* Delta-class GST (bmGSTD), Sigma-class GST (bmGSTS) and unclassified GST (bmGSTu) were determined [11–13]. Because the silkworm provides a model for studying Lepidopterans [14,15], comprehensive research on silkworm GSTs should provide insights into combating those species considered as agricultural pests.

We found that the mRNA encoding an Omega-class GST of *B. mori* (bmGSTO) is induced after exposure to various environmental stresses such as bacteria, ultraviolet-B light, and three commonly used chemical insecticides [8,16]. Further, bmGSTO exhibits dehydroascorbate (DHA) reductase, GSH peroxidase, thiol transferase, and GST activity [16]. GSH peroxidase functions as an antioxidant by catalyzing the reduction of harmful peroxides by GSH and protects lipid membranes and other cellular components against oxidative stress. Thiol transferase is responsible for GSH homeostasis by catalyzing the peroxidation reaction of GSH, resulting in the production of oxidized glutathione. Evidence indicates that bmGSTO plays a role in scavenging reactive oxygen species through its peroxidase activity and induces resistance to oxidative stress mediated by its DHA reductase and thiol transferase activities [16].

To understand better the molecular basis for substrate recognition and catalysis by the enzyme, we report here the three-dimensional crystal structure of recombinant bmGSTO and the structure–function relationships involved in its catalytic action.

2. Materials and methods

2.1. Protein crystallization and analysis

A cDNA encoding bmGSTO [8] was inserted into the vector pET-11b (Novagen) and used to transform *Escherichia coli* strain BL21 (DE3) (TAKARA). Recombinant bmGSTO was purified according to published methods [8,16] using ammonium sulfate fractionation, ion-exchange chromatography, and gel filtration chromatography, and then concentrated using a centrifugal filter (Millipore) to approximately 10 mg/ml in 20 mM Tris–HCl buffer, pH 8.5, containing 0.2 M NaCl. bmGSTO was co-crystalized with 10 mM GSH using the sitting-drop vapor diffusion method at 20 °C using Crystal Screen Kits (Hampton Research), including PEG/Ion-1 and -2,

Abbreviations: GSH, glutathione; GST, glutathione transferase; GSTO, Omega-class GST; SDS–PAGE, sodium dodecyl sulfate–polyacrylamide gel electrophoresis.

* Corresponding author. Fax: +81 92 624 1011.
E-mail address: yamamok@agr.kyushu-u.ac.jp (K. Yamamoto).

0006-291X/$ - see front matter © 2013 Elsevier Inc. All rights reserved.
http://dx.doi.org/10.1016/j.bbrc.2013.08.011

Crystal Screen-1 and -2, and Cryo-1 and -2, as reservoir solutions. Each drop was formed by mixing an equal (0.2 μl) or two fold greater volume of protein and reservoir solutions, respectively. Crystals suitable for X-ray analysis were grown for 3 months in 0.2 M potassium iodide and 20% PEG3350 (w/v).

X-ray diffraction data were acquired with cryo-cooled crystals using synchrotron radiation at beamlines BL-5A at the Photon Factory (The High Energy Accelerator Research Organization, Tsukuba, Japan) and BL44XU in the SPring-8 (Japan Synchrotron Radiation Research Institute (JASRI), Hyogo, Japan) under cryogenic conditions. Crystals were scooped with a nylon loop and transferred to cryoprotectant solution containing 25% (v/v) ethylene glycol before freezing in liquid nitrogen. The diffraction data were collected from a single crystal at 90 K in a stream of nitrogen gas and were processed using the programs *DENZO* and *SCALEPACK* as implemented in *HKL-2000* program package [17].

2.2. Determination of structure

The initial phase of bmGSTO was determined using the molecular replacement method aided by the program *MOLREP* [18] using the human Omega-class GST (hGSTO1-1, PDB ID: 1EEM[19]) as a search model. The structures of bmGSTO complexed with GSH were refined using the program *PHENIX* [19] against the data from 32.8 to 2.5 Å. Manual adjustments of the structure were carried out using the program *Coot* [20]. The stereochemical quality of the final model was assessed using the program *MolProbity* [21]. Crystallographic parameters and refinement statistics are summarized in Table 1. Figures were prepared using the program *PyMOL* (http://pymol.sourceforge.net).

The atomic structure of bmGSTO complexed with GSH has been deposited in the Protein Data Bank (PDB ID: 3WD6). Alignment of deduced amino acid sequences was performed using GENETYX-MAC (ver. 14.0.12).

2.3. Measurements of enzyme activity

Recombinant wild-type bmGSTO was overexpressed and purified as described above. Final protein preparations were subjected to SDS–PAGE using a 15% polyacrylamide slab gel containing 0.1% SDS [22] followed by staining with Coomassie Brilliant Blue R250. Protein concentration was measured using a Protein Assay Kit (Bio-Rad Laboratories) with bovine serum albumin as a standard. GST activity using the substrates 1-chloro-2,4-dinitrobenzene (CDNB) and GSH was measured spectrophotometrically [11]. Briefly, 0.01 ml of test solution was added to 1 ml of 50 mM sodium phosphate buffer, pH 6.5, containing 0.5 mM CDNB and 5 mM GSH. Changes in absorbance (340 nm/min) were monitored at 30 °C and converted into moles CDNB conjugated/min/mg protein using the molar extinction coefficient of the resultant 2,4-dinitrophenylglutathione (ε340 = 9600 M^{-1} cm^{-1}). Alternatively, 4-hydroxynonenal (4-HNE), ethacrynic acid, or 4-nitrophenyl acetate was used instead of CDNB. The concentrations of substrates were varied to determine kinetic parameter (K_m), which were calculated using a nonlinear least-squares data-fitting algorithm (KaleidaGraph, Synergy Software). Thiol transferase activity was measured using hydroxyethyl disulfide as a substrate [23], and glutathione-dependent DHA reductase activity was determined spectrophotometrically with DHA [23]. GSH peroxidase activity was measured by determining the oxidation of NADPH at OD_{340} in the presence of GSH, glutathione reductase, and H_2O_2 as substrates [24].

2.4. Site-directed mutagenesis

Amino acid-substitution mutants of bmGSTO were constructed using a plasmid containing the coding sequences of wild-type bmGSTO and the Quick-Change Site-Directed Mutagenesis Kit (Agilent Technologies, Wilmington, DE, USA) according to the manufacturer's recommendations. The nucleotide sequence of the full-length mutant cDNA was determined by DNA sequencing. Sequence alignments were performed using GENETYX-MAC (ver. 14.0.12, GENETYX Corporation).

Table 1
Data collection and refinement statistics.

Parameter	bmGSTO
Space group	$P22_12_1$
Unit cell parameters (Å)	a = 75.86, b = 89.89, c = 182.2
Beam line	PF BL-5A
Wavelength (Å)	1.0
Resolution range (Å)	32.8–2.50 (2.64–2.50)
Total number of observation reflections	224,155 (6843)
Total number of unique reflections	43,880 (1522)
Multiplicity	4.5 (5.1)
R_{merge}[a] (%)	4.1 (11.0)
$\langle I\rangle/\langle\sigma(I)\rangle$[b]	30.0 (12.5)
Completeness (%)	98.4 (99.8)
Refinement statistics	
Resolution range (Å)	32.8–2.50
Number of reflections	
Working set/Test set	83,052/4160
R_{work}[c] (%)/R_{free}[d] (%)	20.8/25.6
Root-mean-square deviations	
Bond lengths (Å)/bond angles (°)	0.009/1.088
Average B-factors (Å^2)/number of atoms	
Protein	41.0/7963
Small molecules[e]	36.8/117
Water	32.6/342
Ramachandran plot	
Preferred regions (%)	95.9
Allowed regions (%)	3.2
Outliers (%)	0.9

[a] $R_{merge} = \sum(I - \langle I\rangle)/\sum\langle(I)\rangle$,where I is the intensity measurement for a given reflection and $\langle I\rangle$ is the average intensity for multiple measurements of this reflection.
[b] Values in parentheses indicate the highest-resolution shell.
[c] $R_{work} = \sum|F_{obs} - F_{cal}|/\sum F_{obs}$, where F_{obs} and F_{cal} are observed and calculated structure-factor amplitudes.
[d] R_{free} value was calculated using only an unrefined, randomly chosen subset of reflection data (5%) that were excluded from refinement.
[e] Small molecules include glutathione, iodide ion, potassium ion, polyethylene glycol and 1,2-propanediol.

3. Results and discussion

3.1. Structural determination and refinement

The substrate specificity of GST is conferred by the G-site (where GSH binds) and the H-site (where the hydrophobic substrate binds). The diversity of amino acids at both GST binding sites is associated with substrate selectivity.

The crystallographic space group is $P22_12_1$ with unit cell dimensions of a = 75.86 Å, b = 89.89 Å, and c = 182.2 Å. The final X-ray diffraction data and structural refinement statistics are presented in Table 1. The structural refinement against the data up to 2.5 Å resolution converged to an R_{work} factor of 20.8% and R_{free} factor of 25.6%. The root-mean-square deviations for bond lengths and angles are 0.009 Å and 1.088°, respectively. In Ramachandran plot 95.9% of the residues were located in the most preferred regions, 3.2% in the allowed regions, and 0.9% in the outlier regions.

3.2. Crystal structure of bmGSTO

The crystal structure of bmGSTO was solved using the molecular replacement method. This *B. mori* protein shares 40% sequence

identity with the query model human GSTO1-1 (hGSTO1-1) [PDB ID: 1EEM]. Secondary structural elements of bmGSTO were defined using the DSSP program [25]. Each bmGSTO monomer includes 10 α-helices as follows: α1 (residues 39–50), α2 (residues 69–72), α3 (residues 92–102), α4 (residues 113–124), α5 (residues 127–138), α6 (residues 145–165), α7 (residues 177–189), α8 (residues 206–216), α9 (residues 219–222) and α10 (residues 228–238). The locations of the four β-strands are as follows: β1 (residues 30–34), β2 (residues 55–60), β3 (residues 80–84) and β4 (residues 87–90) (Fig. 1). Its globular shape is similar to other Omega-class GSTs [26–28]. The structure can be divided into two major domains. The N-terminal thioredoxin-like domain comprises four β-strands and 2α-helices, whereas the other α-helices are located in the C-terminal domain. The N-terminal domain resembles the typical ββαβαβ motif of a thioredoxin fold and has a unique extension of unknown function (Fig. 1) compared with other cytosolic GSTs.

The bmGSTO amino acid sequence is 40% and 36%, and 30% identical to those of hGSTO1-1 and human GSTO2-2 (hGSTO2-2) (PDB ID: 3Q18), respectively. We found that the secondary structures of bmGSTO and hGSTO1-1 and hGSTO2-2 are highly conserved (data not shown). According to the *B. mori* draft genome sequence, there are at least four Omega-class GSTs. For one of the *B. mori* isozymes (bmGSTO3-3)[26], the crystal structure was analyzed (PDB ID: 3RBT). The bmGSTO amino acid sequence is 30% identity to that of bmGSTO3-3. The structural comparison with bmGSTO3-3 reveals that one helix (from 183 to 216) is specific to bmGSTO3-3, but it is not present between α7 and α8 of bmGSTO (Fig. 2).

3.3. Amino acid residues responsible for catalysis

Comparison between bmGSTO and hGSTO1-1 shows a prominent cleft between N-terminal and C-terminal domains (Fig. 1). The liganded bmGSTO structure shows that GSH is present in the active site located in the deep cleft between the two domains (Fig. 1). Each monomer in dimer has one molecule of GSH in the active site. The active site can be divided into two subsites, the G-site and the H-site. The GSH–bmGSTO structure indicates that GSH is tightly secured in the G-site formed by the residues Cys38, Pro39, Tyr40, Arg43, Leu62, Lys65, Lys77, Val78, Glu91 and Ser92 of bmGSTO (Fig. 3); these are superimposed on the corresponding residues of hGSTO1-1 as follows: Cys32, Pro33, Phe34, Arg37, Leu56, Lys59, Leu71, Val72, Glu85 and Ser86.

GSH binds to the G-site with its γ-glutamyl region forming hydrogen bonds with the side chain of Glu91 (Glu85 in hGSTO1-1), the hydroxyl group, and the main chain of Ser92 (Ser86 in hGSTO1-1) (Fig. 3). The cysteinyl moiety of GSH forms a mixed disulfide bond with the side chain of Cys38 (Cys32 in hGSTO1-1) and forms hydrogen bonds with the Lys77 (Leu71 in hGSTO1-1) backbone and the side chain of Val78 (Val72 in hGSTO1-1) (Fig. 3). The glycyl moiety of GSH interacts with the side-chain of Lys65 (Lys59 in hGSTO1-1). Arg37 in hGSTO1-1 forms a salt bridge with the glycyl moiety of GSH. The equivalent Arg43 in bmGSTO is far to form the salt bridge (Fig. 3). Our results reveal that GSH tightly binds to the GSH-binding site (G-site) of bmGSTO. We compared the structures of bmGSTO with those of the hGSTO2-2 and bmGSTO3-3 and found that the G-site of hGSTO2-2 is similar (7/9 and 5/9 G-site residues are present in hGSTO2-2 and bmGSTO3-3, respectively).

Winayanuwattikun and Ketterman [29] proposed that the electron-sharing network contributes to the catalytic activity of GST and can be divided into networks called type I and II [29]. The type I networks, exemplified by the GSTs of Delta, Theta, Omega and Tau classes, contain an acidic amino acid residue at position 64, whereas the type II networks (GSTs of Alpha, Mu and Pi classes) have a polar amino acid residue (glutamate) capable of interacting with the γ-glutamyl portion of GSH. Glu91 is conserved in the sequence of bmGSTO, which resembles a member of the type I network. In bmGSTO, Arg43, Glu91 and Ser92 could participate in the electron sharing network, which is characteristic of Omega-class GST type I networks.

The G-site resides in the N-terminal domain of each monomer (Fig. 3) bind 1 molecule of GSH inside the pocket formed by residues Cys38, Pro39, Tyr40, Arg43, Leu62, Lys65, Lys77, Val78,

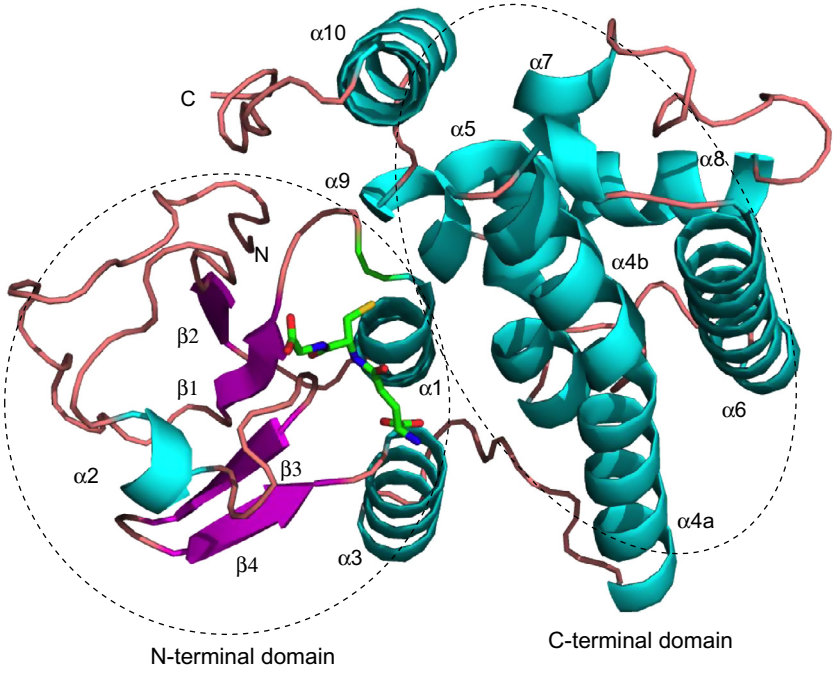

Fig. 1. Tertiary structure of bmGSTO. The α-helices and β-strands are indicated by magenta and blue and labeled with α and β. N-terminal and C-terminal amino acid residues are indicated N and C. Carbon atoms in GSH are green. Colors of other atoms are as follows: oxygen (red), nitrogen (blue), and sulfur (yellow). N- and C-terminal domains are indicated by the dashed circles. (For interpretation of the references to color in this figure legend, the reader is referred to the web version of this article.)

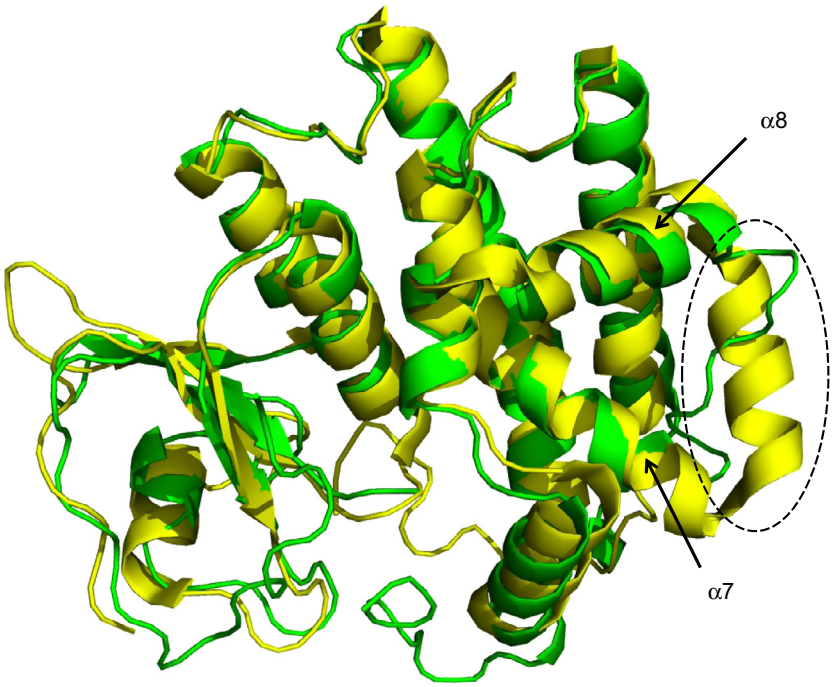

Fig. 2. Tertiary structure superposition of bmGSTO with bmGSTO3-3. The carbon atoms of the amino acid residues of bmGSTO and bmGSTO3-3 are green and yellow, respectively. The location of α-helix (from 183 to 216) in bmGSTO3-3 is indicated by the dashed circle. (For interpretation of the references to color in this figure legend, the reader is referred to the web version of this article.)

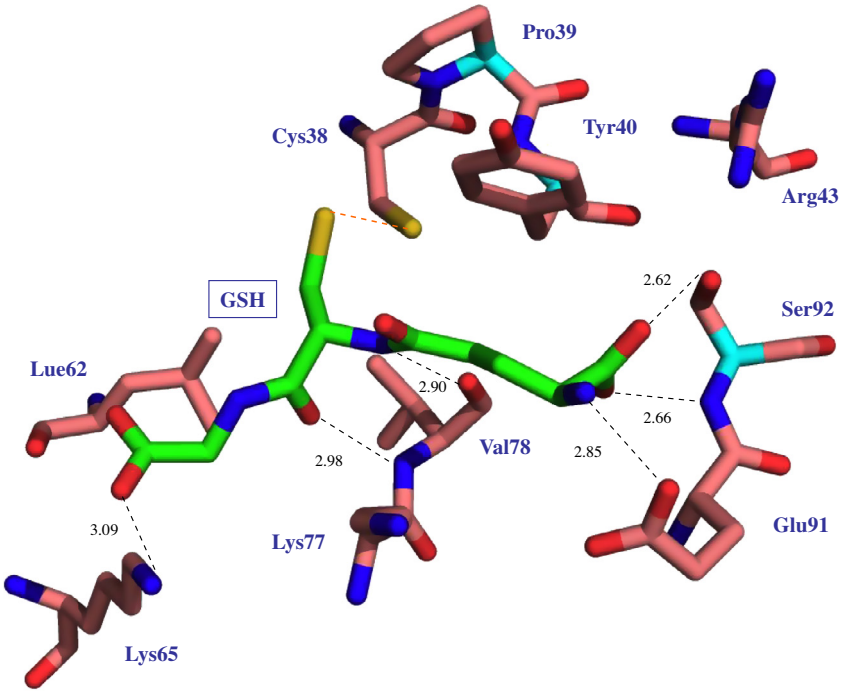

Fig. 3. Amino acid residues near the G-site of bmGSTO. Coloring schemes for GSH are as described in the legend for Fig. 1. The carbon atoms of the amino acid residues of bmGSTO are pink. Colors of other atoms are as follows: oxygen (red), nitrogen (blue), and sulfur (yellow). Hydrogen bonds are indicated by black dotted lines. The dashed orange line indicates a mixed disulfide bond. (For interpretation of the references to color in this figure legend, the reader is referred to the web version of this article.)

Glu91 and Ser92 of bmGSTO (Fig. 3). To determine which residues contribute to the catalytic activity of bmGSTO, five residues were converted to Ala by using site-directed mutagenesis, and the resulting mutants were named K65A, K77A, V78A, E91A and S92A, respectively. SDS–PAGE analysis revealed that each protein migrated as a single band. The K_m values of the bmGSTO mutants were compared with those of the wild-type enzyme using CDNB as substrate (Table 2). The most prominent change was the diminished affinities of E91A and V78A. The bmGSTO exhibited DHA reductase, GSH peroxidase, and thiol transferase activities. The

Table 2
Comparison of kinetic data (K_m) for bmGSTO against various substrates.

	Wild	K65A	K77A	V78A	E91A	S92A
CDNB	0.67 (0.06)[a]	0.85 (0.06)	0.39 (0.04)	1.42 (0.12)	4.77 (0.55)	0.31 (0.03)
4-HNE	0.006 (0.001)[a]	NA	NA	NA	NA	NA
Thiol transferase	0.15 (0.03)[a]	NA	NA	NA	NA	NA
DHA reductase	0.64 (0.08) [a]	NA	NA	NA	NA	NA
GSH peroxidase	0.32 (0.05) [a]	NA	NA	NA	NA	NA

[a] These values were obtained previously (Yamamoto et al., 2010). The value of K_m is expressed as the mean (SD) of three independent experiments. K_m is expressed as mM. NA means "undetectable activity". CDNB, 1-chloro-2,4-dinitrobenzene; 4-HNE, 4-hydroxynonenal; DHA, dehydroascorbate; GSH, glutathione.

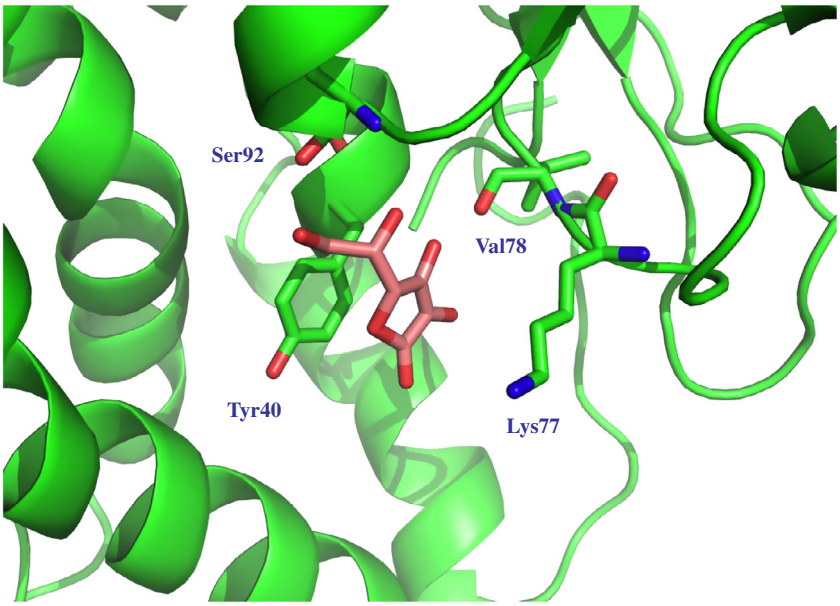

Fig. 4. Putative ascorbic acid binding sites. Carbon atoms in bmGSTO are green. Colors of other atoms are as follows: oxygen (red) and nitrogen (blue). Ascorbic acid is shown in magenta. (For interpretation of the references to color in this figure legend, the reader is referred to the web version of this article.)

K_m values with the substrate 4-HNE, and the thiol transferase, DHA reductase, and GSH peroxidase activities of all mutants were significantly low (Table 2).

3.4. Putative substrate-binding sites

The superposition of the backbones of bmGSTO and hGSTO1-1 revealed that both possess an N-terminal domain that includes the G-site as well as a C-terminal domain that includes the H-site. Their secondary structures are comparable, particularly at the G-site. Variations in H-site structures of GSTs are responsible for their different substrate specificities. The H-site of hGSTO1-1 contains Phe31, Cys32, Pro33, Arg184, Met187, Trp222, Phe225, Leu226 and Tyr229 [27]. In the sequence of bmGSTO, we found that 5 residues, Cys38, Pro39, Arg188, Phe234 and Tyr238 correspond to those of hGSTO1-1. The proline following this cysteine, as Pro39 follows Cys38 of bmGSTO, promotes optimal positioning of the Cys38 thiol for stabilizing the thiolate form [27]. We found that bmGSTO included a conserved amino acid residue (Cys38) in the G-site, which is one of specific features of Omega-GSTs. This Cys residue, which is essential for catalysis, is absent in another silkworm Omega-class GST isozyme (bmGSTO3-3). The Cys residue was replaced by Asn residues in bmGSTO3-3, suggesting that the bmGSTO3-3 H-site differs. When the H-site of hGSTO2-2 (Phe31, Cys32, Pro33, Arg184, Tyr188, Phe223, Phe226, Leu227 and Tyr230) is co-localized with the equivalent site in bmGSTO, we also found that the five residues corresponded in their positions.

The structure of the hGSTO1-1-C32S mutant with ascorbic acid (AA) (PDB ID: 3VLN) has been determined [28]. Superposition between hGSTO1-1-C32S and bmGSTO reveal that the stacking interaction of AA with Tyr40 could be observed in the structure of bmGSTO (Fig. 4). Tyr40 of bmGSTO occupies the G-site that typically binds the γ-glutamyl moiety of GSH. AA could contact the side chain of Lys77, the side-chain hydroxyl of Ser92, and the backbone carbonyl of Val78 in bmGSTO. The reduction of DHA to AA is a vital cellular function. AA plays a major role in scavenging free radicals and specific reactive oxygen species [30]. The results suggest that bmGSTO functions to regulate the redox balance. Two isozymes (hGSTO1-1 and hGSTO2-2) with DHA reductase activity are expressed by human [28]. The structure of a human GSTO1-1–AA complex has been determined [28]. AA stacks against a conserved aromatic residue, Phe34 (equivalent to Tyr40 in bmGSTO). Mutation of Y34 to alanine in hGSTO2-2 eliminates DHA reductase activity [28].

We determined the tertiary-structure of bmGSTD, bmGSTS and bmGSTu [11–13]. Comparison of bmGSTO to other *B. mori* GSTs showed that their secondary structures, including α-helices and β-strands, were similar. There is a difference in the number of α-helices as follows: eight in bmGSTD and bmGSTu, nine in bmGSTS, and ten in bmGSTO. The identity between bmGSTO and other *B. mori* GSTs is 21.8% (bmGSTD), 19.6% (bmGSTS), and 19.0% (bmGSTu). In the GST G-site, certain amino acid residues are conserved among the silkworm GSTs. The residues that interact with the γ-glutamyl region of GSH, Arg43, Glu91 and Ser92 were conserved. The cysteinyl moiety of GSH interacts with the con-

served Val73 and catalytic residue, Cys38, of bmGSTO. The cysteine residue in the N-terminal region is catalytically essential and is well conserved in Omega-class GSTs, although bmGSTO3-3 has Asn the corresponding residue in place of Cys. Serine is a crucial residue for sigma-class GST activity, and it is replaced by Tyr in theta-class GSTs [27,28]. The catalytic residue is GST-class specific; Ser for bmGSTu and bmGSTD, and Tyr for bmGSTS. The Lys65 residue that interacts with the glycyl moiety of GSH is replaced by Trp39 in bmGSTS, by His52 in bmGSTu and by His53 in bmGSTD. Gln52 in bmGSTu and Gln51 in bmGSTD, and Trp39 in bmGSTS also form hydrogen bonds with the glycyl moiety of GSH, whereas the equivalent residue is not present in bmGSTO. Compared with the G-sites, the GST H-sites are structurally diverse. Thus, the higher-order features among GSTs are similar, whereas the H-sites are GST-class specific, which likely affects their substrate specificity.

In summary, we describe here the crystal structure of a bmGSTO and reconstructed its entire architecture by comparing it with the three-dimensional structure of its human homolog. By preparing bmGSTO–GSH complexes and generating mutant enzyme, we identified the amino acid residues involved in catalysis. We are currently pursuing co-crystallization of bmGSTO with a suitable inhibitor-GSH conjugate to aid in the rational design of more effective pesticides.

Acknowledgments

This work was supported in part by a Grant-in-Aid for Scientific Research from the Ministry of Education, Science, Sports and Culture of Japan. The work was also supported in part by a Research Grant for Young Investigators of Faculty of Agriculture, Kyushu University. This work was performed under the auspices of the Cooperative Research Program of Institute for Protein Research, Osaka University. The synchrotron radiation experiments were carried out at the BL-5A of Photon Factory (Proposal No. 2012G003) and at the BL44XU of SPring-8 with the approval of JASRI (Proposal Nos. 2012A6756, and 2012B6756).

References

[1] I. Listowsky, M. Abramovitz, H. Homma, Y. Niitsu, Intracellular binding and transport of hormones and xenobiotics by glutathione-S-transferases, Drug Metab. Rev. 19 (1988) 305–318.
[2] R.N. Armstrong, Structure, catalytic mechanism, and evolution of the glutathione transferases, Chem. Res. Toxicol. 10 (1997) 2–18.
[3] B. Mannervik, P.G. Board, J.D. Hayes, I. Listowsky, W.R. Pearson, Nomenclature for mammalian soluble glutathione transferases, Methods Enzymol. 401 (2005) 1–8.
[4] C.P. Tu, B. Akgul, Drosophila glutathione S-transferases, Methods Enzymol. 401 (2005) 204–226.
[5] K. Yamamoto, P. Zhang, F. Miake, N. Kashige, Y. Aso, Y. Banno, H. Fujii, Cloning, expression and characterization of theta-class glutathione S-transferase from the silkworm, *Bombyx mori*, Comp. Biochem. Physiol. B: Biochem. Mol. Biol. 141 (2005) 340–346.
[6] K. Yamamoto, P.B. Zhang, Y. Banno, H. Fujii, Identification of a sigma-class glutathione-S-transferase from the silkworm, *Bombyx mori*, J. Appl. Entomol. 130 (2006) 515–522.
[7] K. Yamamoto, H. Fujii, Y. Aso, Y. Banno, K. Koga, Expression and characterization of a sigma-class glutathione S-transferase of the fall webworm, *Hyphantria cunea*, Biosci. Biotechnol. Biochem. 71 (2007) 553–560.
[8] K. Yamamoto, S. Nagaoka, Y. Banno, Y. Aso, Biochemical properties of an omega-class glutathione S-transferase of the silkmoth, *Bombyx mori*, Comp. Biochem. Physiol. C: Toxicol. Pharmacol. 149 (2009) 461–467.
[9] K. Yamamoto, Y. Shigeoka, Y. Aso, Y. Banno, M. Kimura, T. Nakashima, Molecular and biochemical characterization of a Zeta-class glutathione S-transferase of the silkmoth, Pestic. Biochem. Physiol. 94 (2009) 30–35.
[10] K. Yamamoto, H. Ichinose, Y. Aso, Y. Banno, M. Kimura, T. Nakashima, Molecular characterization of an insecticide-induced novel glutathione transferase in silkworm, Biochim. Biophys. Acta 2011 (1810) 420–426.
[11] Y. Kakuta, K. Usuda, T. Nakashima, M. Kimura, Y. Aso, K. Yamamoto, Crystallographic survey of active sites of an unclassified glutathione transferase from *Bombyx mori*, Biochim. Biophys. Acta 2011 (1810) 1355–1360.
[12] K. Yamamoto, K. Usuda, Y. Kakuta, M. Kimura, A. Higashiura, A. Nakagawa, Y. Aso, M. Suzuki, Structural basis for catalytic activity of a silkworm Delta-class glutathione transferase, Biochim. Biophys. Acta 2012 (1820) 1469–1474.
[13] K. Yamamoto, A. Higashiura, M. Suzuki, K. Aritake, Y. Urade, N. Uodome, A. Nakagawa, Crystal structure of a *Bombyx mori* sigma-class glutathione transferase exhibiting prostaglandin E synthase activity, Biochim. Biophys. Acta 2013 (1830) 3711–3718.
[14] K. Mita, M. Morimyo, K. Okano, Y. Koike, J. Nohata, H. Kawasaki, K. Kadono-Okuda, K. Yamamoto, M.G. Suzuki, T. Shimada, M.R. Goldsmith, S. Maeda, The construction of an EST database for *Bombyx mori* and its application, Proc. Natl. Acad. Sci. USA 100 (2003) 14121–14126.
[15] K. Mita, M. Kasahara, S. Sasaki, Y. Nagayasu, T. Yamada, H. Kanamori, N. Namiki, M. Kitagawa, H. Yamashita, Y. Yasukochi, K. Kadono-Okuda, K. Yamamoto, M. Ajimura, G. Ravikumar, M. Shimomura, Y. Nagamura, I.T. Shin, H. Abe, T. Shimada, S. Morishita, T. Sasaki, The genome sequence of silkworm, *Bombyx mori*, DNA Res. 11 (2004) 27–35.
[16] K. Yamamoto, S. Teshiba, Y. Shigeoka, Y. Aso, Y. Banno, T. Fujiki, Y. Katakura, Characterization of an omega-class glutathione S-transferase in the stress response of the silkmoth, Insect Mol. Biol. 20 (2011) 379–386.
[17] Z. Otwinowski, W. Minor, Processing of X-ray diffraction data collected in oscillation mode, Methods Enzymol. 276 (1997) 307–326.
[18] A. Vagin, A. Teplyakov, An approach to multi-copy search in molecular replacement, Acta Crystallogr. D: Biol. Crystallogr. 56 (2000) 1622–1624.
[19] P.D. Adams, P.V. Afonine, G. Bunkoczi, V.B. Chen, N. Echols, J.J. Headd, L.W. Hung, S. Jain, G.J. Kapral, R.W. Grosse Kunstleve, A.J. McCoy, N.W. Moriarty, R.D. Oeffner, R.J. Read, D.C. Richardson, J.S. Richardson, T.C. Terwilliger, P.H. Zwart, The Phenix software for automated determination of macromolecular structures, Methods 55 (2011) 94–106.
[20] P. Emsley, K. Cowtan, Coot: model-building tools for molecular graphics, Acta Crystallogr. D: Biol. Crystallogr. 60 (2004) 2126–2132.
[21] V.B. Chen, W.B. Arendall 3rd, J.J. Headd, D.A. Keedy, R.M. Immormino, G.J. Kapral, L.W. Murray, J.S. Richardson, D.C. Richardson, MolProbity: all-atom structure validation for macromolecular crystallography, Acta Crystallogr. D: Biol. Crystallogr. 66 (2010) 12–21.
[22] U.K. Laemmli, Cleavage of structural proteins during the assembly of the head of bacteriophage T4, Nature 227 (1970) 680–685.
[23] A.K. Whitbread, A. Masoumi, N. Tetlow, E. Schmuck, M. Coggan, P.G. Board, Characterization of the omega class of glutathione transferases, Methods Enzymol. 401 (2005) 78–99.
[24] F.F. Chu, J.H. Doroshow, R.S. Esworthy, Expression, characterization, and tissue distribution of a new cellular selenium-dependent glutathione peroxidase, GSHPx-GI, J. Biol. Chem. 268 (1993) 2571–2576.
[25] R. Maiti, G.H.V. Domselaar, H. Zhang, D.S. Wishart, SuperPose: a simple server for sophisticated structural superposition, Nucleic Acids Res. 1 (2004) W590–W594.
[26] B.Y. Chen, X.X. Ma, P.C. Guo, X. Tan, W.F. Li, J.P. Yang, N.N. Zhang, Y. Chen, Q. Xia, C.Z. Zhou, Structure-guided activity restoration of the silkworm glutathione transferase Omega GSTO3-3, J. Mol. Biol. 412 (2011) 204–211.
[27] P.G. Board, M. Coggan, G. Chelvanayagam, S. Easteal, L.S. Jermiin, G.K. Schulte, D.E. Danley, L.R. Hoth, M.C. Griffor, A.V. Kamath, M.H. Rosner, B.A. Chrunyk, D.E. Perregaux, C.A. Gabel, K.F. Geoghegan, J. Pandit, Identification, characterization, and crystal structure of the Omega class glutathione transferases, J. Biol. Chem. 275 (2000) 24798–24806.
[28] H. Zhou, J. Brock, D. Liu, P.G. Board, A.J. Oakley, Structural insights into the dehydroascorbate reductase activity of human omega-class glutathione transferases, J. Mol. Biol. 420 (2012) 190–203.
[29] P. Winayanuwattikun, A.J. Ketterman, Glutamate-64, a newly identified residue of the functionally conserved electron-sharing network contributes to catalysis and structural integrity of glutathione transferases, Biochem. J. 402 (2007) 339–348.
[30] B. Frei, L. England, B.N. Ames, Ascorbate is an outstanding antioxidant in human blood plasma, Proc. Natl. Acad. Sci. USA 86 (1989) 6377–6381.